journal

J. Am. Ceram. Soc., **85** [1] 245–52 (2002)

Novel Two-Step Sintering Process to Obtain a Bimodal Microstructure in Silicon Nitride

Hai-Doo Kim,* Byung-Dong Han, Dong-Soo Park,* Byong-Taek Lee,† and Paul F. Becher*,‡

Ceramic Materials Group, Korea Institute of Machinery and Materials, Kyungnam 641–010, Korea;
Division of Advanced Materials Engineering, Kongju National University, Kongju City 314–701, Korea; and
Metals and Ceramics Division, Oak Ridge National Laboratory, Oak Ridge, Tennessee 37831–6068

A two-step sintering process is described in which the first step suppresses densification while allowing the α-to-β phase transformation to proceed, and the second step, at higher temperatures, promotes densification and grain growth. This process allows one to obtain a bimodal microstructure in Si_3N_4 without using β-Si_3N_4 seed crystals. A carbothermal reduction process was used in the first step to modify the densification and transformation rates of the compacts consisting of Si_3N_4, Y_2O_3, Al_2O_3, and a carbon mixture. The carbothermal reduction process reduces the oxygen:nitrogen ratio of the Y-Si-Al-O-N glass that forms, which leads to the precipitation of crystalline oxynitride phases, in particular, the apatite phase. Precipitation of the apatite phase reduces the amount of liquid phase and retards the densification process up to 1750°C; however, the α-to-β phase transformation is not hindered. This results in the distribution of large β-nuclei in a porous fine-grained β-Si_3N_4 matrix. Above 1750°C, liquid formed by the melting of apatite resulted in a rapid increase in densification rates, and the larger β-nuclei also grew rapidly, which promoted the development of a bimodal microstructure.

I. Introduction

SILICON NITRIDE is one of the candidate materials for the high-temperature structural applications; however, the mechanical properties have not reached their full potential. One of the methods to improve strength and fracture toughness is to produce a bimodal microstructure in which large elongated grains in a fine matrix act as reinforcing grains, which contribute to crack-bridging toughening mechanisms.[1–5] To promote the formation of a bimodal microstructure, β-Si_3N_4 seed crystals have been used.[6–15] A number of approaches have been discussed to synthesize such β-Si_3N_4 seed crystals with different morphologies.[16–19] The addition of β-Si_3N_4 seed crystals to either a mixture of fine α-Si_3N_4 powder and sintering additives,[6–10,14–16] or a mixture of β-Si_3N_4 powder and sintering additives,[11–13] has been shown to be quite effective for producing the desired bimodal microstructure.

This addition of larger β-Si_3N_4 seed crystals dominates the formation of larger elongated grains.[20] In the absence of β-seeds, the formation of a bimodal microstructure is hampered by concurrent activities involving phase transformation, grain growth, and densification. Moreover, the α-to-β phase transformation occurs over a wide temperature range (e.g., 1450° to 1750°C) where the nucleation and growth of β-Si_3N_4 grains can proceed in an uncontrolled manner and produce a broad grain size distribution rather than a distinct bimodal one. Because densification is always accompanied by grain growth, Mitomo[21] suggested that densification be separated from grain growth to obtain a bimodal microstructure. His processing approach involved the completion of densification before significant phase transformation, followed by annealing to affect the phase transformation and grow the reinforcing grains. Goto *et al.*[22] manipulated densification and the α-to-β phase transformation by using different sintering additives that generated liquid phases with different viscosities during sintering. Using either 10 wt% Al_2O_3(10A) or a mixture of 1 wt% Y_2O_3 + 6 wt% Al_2O_3(1Y6A) as additives, the densification rates were accelerated relative to those of the α-to-β phase transformation rate. For example, almost full densification was achieved with 10A and 1Y6A additives, while the fraction of the α-to-β phase transformation was only ~30%. However, when a mixture of 5 wt% Y_2O_3 + 2 wt% Al_2O_3(5Y2A) was used, the densification rate was similar to that of the α-to-β phase transformation rate. These two approaches are similar in that they strive to reach full density first, and then complete the transformation and grain growth to achieve a bimodal microstructure.

In this paper, we report on a two-step sintering process to obtain a bimodal microstructure without the addition of special β-Si_3N_4 seed crystals. This is achieved by allowing the phase transformation to proceed while suppressing the densification process using transient solid-phase sintering in the first step, followed by a second step at higher temperatures where the phase melts and promotes densification and selective growth of reinforcing grains.

II. Experimental Procedure

To suppress the densification process, our approach is to reduce the amount of liquid phase present at intermediate temperatures. This can be accomplished by reducing the oxygen content of the powder mixture of α-Si_3N_4 and the sintering additives such as 6 wt% Y_2O_3 and 1 wt% Al_2O_3 using a carbothermal reduction treatment. Two separate batches of 93 wt% α-Si_3N_4 (E-10, Ube Industries, Ltd., Tokyo, Japan), 6 wt% Y_2O_3 (fine, H. C. Starck Co., Berlin, Germany), and 1 wt% Al_2O_3 (AKP-30, Sumitomo Chemical Co., Osaka, Japan) with and without carbon addition (0.5 wt% carbon; activated carbon, Aldrich Chemicals Co., Milwaukee, WI) were prepared. Hereafter, these batches are identified as C-0 and C-0.5, and were formulated to allow us to test the effectiveness of the carbothermal reduction scheme. Each batch was then processed in a planetary ball mill for 20 h using Si_3N_4 balls 5 mm in diameter and methanol in a Si_3N_4 jar. The resultant slurries were dried on a hot plate while stirred, then sieved to −100 +150 mesh, and, finally, isostatically pressed at 250 MPa to form 16 mm disks.

In the first sintering step, the compacts were treated with and without the carbon addition in a tube furnace at 1450°C for 10 h in a flowing nitrogen atmosphere (0.2 L/min) and cooled to room

G. Grathwohl—contributing editor

Manuscript No. 188268. Received September 14, 2000; approved July 26, 2001.
Supported in part by the NRL program of the Korean Ministry of Science and Technology. Author PFB acknowledges the support of the U. S. Department of Energy, Office of Basic Energy Science, Division of Materials Sciences and Engineering, under contract DE-AC05-00-22725 with UT-Battelle, LLC.

*Member, American Ceramic Society.
†Kongju National University.
‡Oak Ridge National Laboratory.

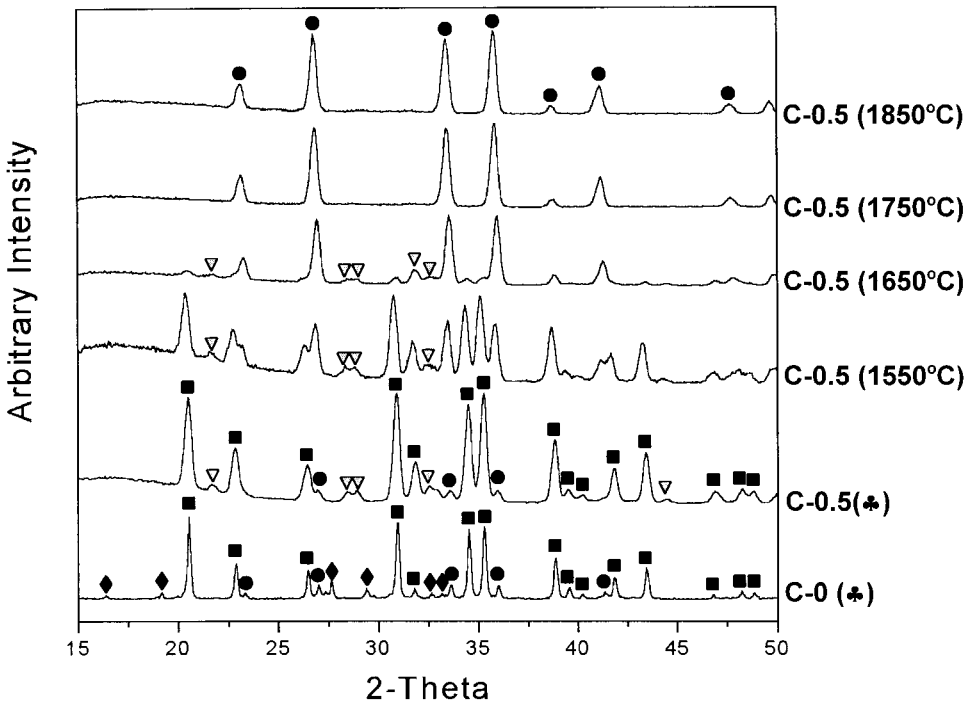

Fig. 1. XRD patterns for the specimens of C-0.5 that have been treated by a carbothermal reduction process at 1450°C for 10 h under a flowing nitrogen atmosphere with increasing temperatures. The lower two patterns (marked) are for C-0 and C-0.5 specimens after the 1st-step sintering procedure at 1450°C for 10 h under a flowing nitrogen atmosphere. XRD JCPDS File Card Nos. 41-0360, 33-1160, 30-1462, and 38-0440 were used to index (■) α-Si_3N_4, (●) β-Si_3N_4, (▽) apatite ($Y_{10}Si_6O_{24}N_2$), and (◆) $Y_2Si_2O_7$, respectively.[46]

temperature by turning off the electric power. The phase contents after the first sintering step of these two compositions were then analyzed. In the second sintering step, compacts were sintered at 1850°C for 3 or 6 h under a 2 MPa nitrogen pressure. The phase development was also characterized in carbothermally treated compacts after sintering at the selected temperatures in the range of 1550° to 1850°C for 0.5 h under 1 MPa of nitrogen.

After the planetary ball-milling, particle size distribution and specific surface area were measured by the laser diffraction method (Model LS-130, Coulter Co., Hialeah, FL) and the BET method (Model ASAP-2010, Micromeritics, Norcross, GA), respectively. Both the oxygen and carbon contents were determined before and after the carbothermal reduction treatment (LECO Co., St. Joseph, MI). Density was measured by the Archimedes method. Phase development was characterized on cross sections of the specimen using XRD (Rigaku Co., Tokyo, Japan). The α:β ratio was calculated using Gazzara's equation.[23] Cross sections were polished to 1 μm with diamond paste and plasma-etched (96% CF_4 + 4% O_2) for microstructural analysis using SEM (Model JSM-5800, JEOL, Tokyo, Japan) and commercially available software (Image Pro 3.0, Media Cybernetics, L.P., Silver Spring, MD). Two different magnifications were used and the grain diameters defined as the largest width were measured for each composition and plotted against the area percentage. More than 1500 grains were measured for each composition.

III. Results

The particle size distributions of the powder mixtures after 20 h of planetary ball-milling have a very narrow particle size distribution (D_{90} = 0.38 μm, D_{50} = 0.22 μm, and D_{10} = 0.13 μm) accompanied by a specific surface area of ~20 m^2/g. The oxygen content of a batch of 93 wt% α-Si_3N_4, 6 wt% Y_2O_3, and 1 wt% Al_2O_3 before milling is 2.9 wt%. Based on an oxygen contribution from the oxide additives of 1.74 wt%, this translates to an oxygen content of 1.16 wt% in the α-Si_3N_4 powder, which is comparable to the nominal composition of 1.23 wt% provided by the manufacturer. The oxygen content of the same batch after a 4 h planetary ball-milling step is 3.5 wt%. The oxygen content of C-0 and C-0.5 batches after 20 h of planetary ball milling is 4.0 and 4.2 wt%, respectively, while those after carbothermal reduction treatment are 4.1 and 3.6 wt%, respectively. The remaining carbon content after the carbothermal reduction ranges from 0.1 to ~0.14 wt%, which is comparable to the carbon content of α-Si_3N_4 starting powder (0.1 wt%). The carbothermal reduction temperature is higher than the Y_2O_3–Al_2O_3–SiO_2 eutectic of 1370°C[24] and, thus, the oxygen content of the resultant Y-Al-Si-O-N glass is lowered.

The XRD patterns shown in Fig. 1 include those for the carbothermally treated C-0.5 specimens, which have been sintered at temperatures in the range of 1550° to 1850°C for 0.5 h under 1 MPa of nitrogen pressure. Moreover, XRD patterns of C-0 and C-0.5 specimens after the 1st-step sintering procedure are shown for comparison (labeled as C-0 and C-0.5, after 1st-step sintering). Note that the C-0 specimen after the 1st-step sintering procedure exhibits mostly α-Si_3N_4 and a small amount of β-Si_3N_4 and $Y_2Si_2O_7$. The carbothermal reduction treatment of the C-0.5 specimen results in α-Si_3N_4 as the major phase and β-Si_3N_4 and apatite as minor phases. The apatite phase in this specimen is thought to precipitate from an oxynitride glass with a low oxygen:nitrogen ratio. The precipitation of the apatite phase is consistent with the subsolidus phase relationships in the Si_3N_4–Y_2O_3–SiO_2 system.[26–29] When the yttrium content remains constant, the phase equilibrium indicates that the compatibility of Si_3N_4 shifts from $Y_2Si_2O_7$ to $Y_{10}(SiO_4)_6N_2$ (apatite) to Y_2SiO_2N (wallastonite), and, finally, to $Y_2Si_3O_3N_4$ (melilite) as the oxygen

Table I. Compositions of C-0.5 in Equivalent Percentage Before and After Carbothermal Reduction Treatment at 1450°C for 10 h in Flowing Nitrogen Atmosphere

	Composition (equiv%)				
	Oxygen	Nitrogen	Silicon	Yttrium	Aluminum
Before	6.179	93.821	97.303	1.970	0.727
After	5.551	94.449	97.308	1.966	0.726

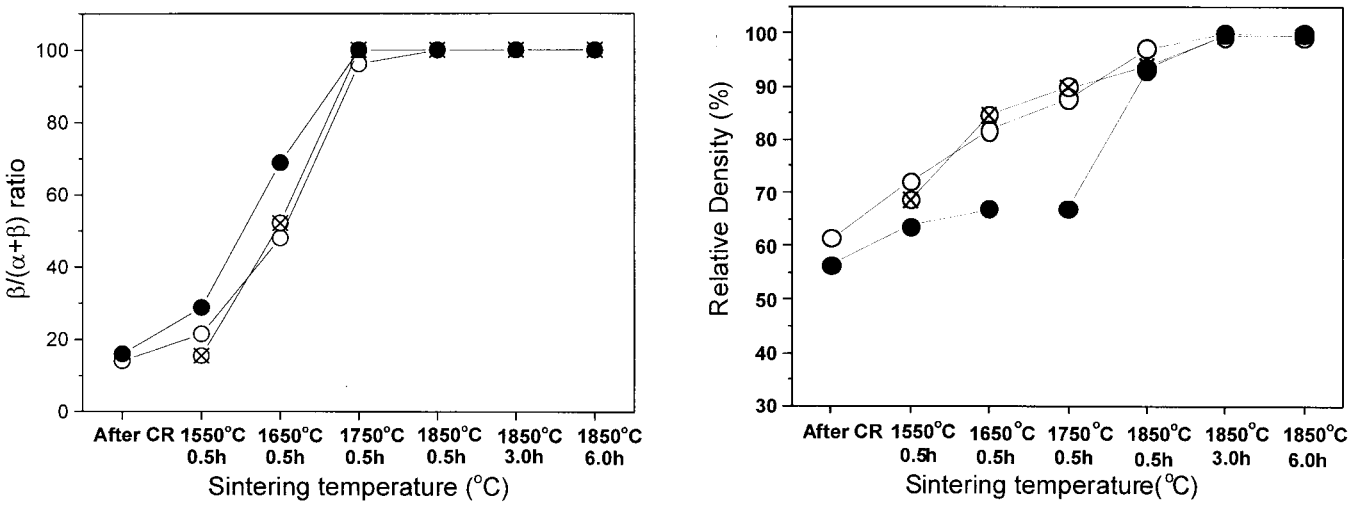

Fig. 2. Phase transformation and densification with increasing sintering temperature and time for specimens of C-0 specimens (⊗) without the 1st-step sintering procedure and (○) with the 1st-step sintering procedure and (●) C-0.5 specimens that have been treated at 1450°C for 10 h under a flowing nitrogen atmosphere. Data points for C-0 specimens without the 1st-step sintering procedure are shown for comparison.

content decreases. For the carbothermally reduced specimen, the decrease in oxygen can shift the composition from the Si_3N_4–$Y_2Si_2O_7$–Si_2N_2O triangle toward the Si_3N_4–$Y_2Si_2O_7$–$Y_{10}(SiO_4)_6N_2$ triangle. Calculated compositions for C-0.5 specimens based on the measured oxygen contents before and after carbothermal reduction treatment (Table I) indicate that the composition shifts toward, but does not reach, the Si_3N_4–$Y_2Si_2O_7$–$Y_{10}(SiO_4)_6N_2$ triangle. However, it does approach the Si_3N_4–$Y_2Si_2O_7$ tie line. It appears that the specimen has not reached the equilibrium condition during carbothermal reduction treatment, and that the apatite phase could have precipitated during cooling.

As seen in Fig. 1, the α-to-β phase transformation continues and the apatite is retained to temperatures of at least 1650°C. At 1750°C, the α-to-β phase transformation reaches completion and

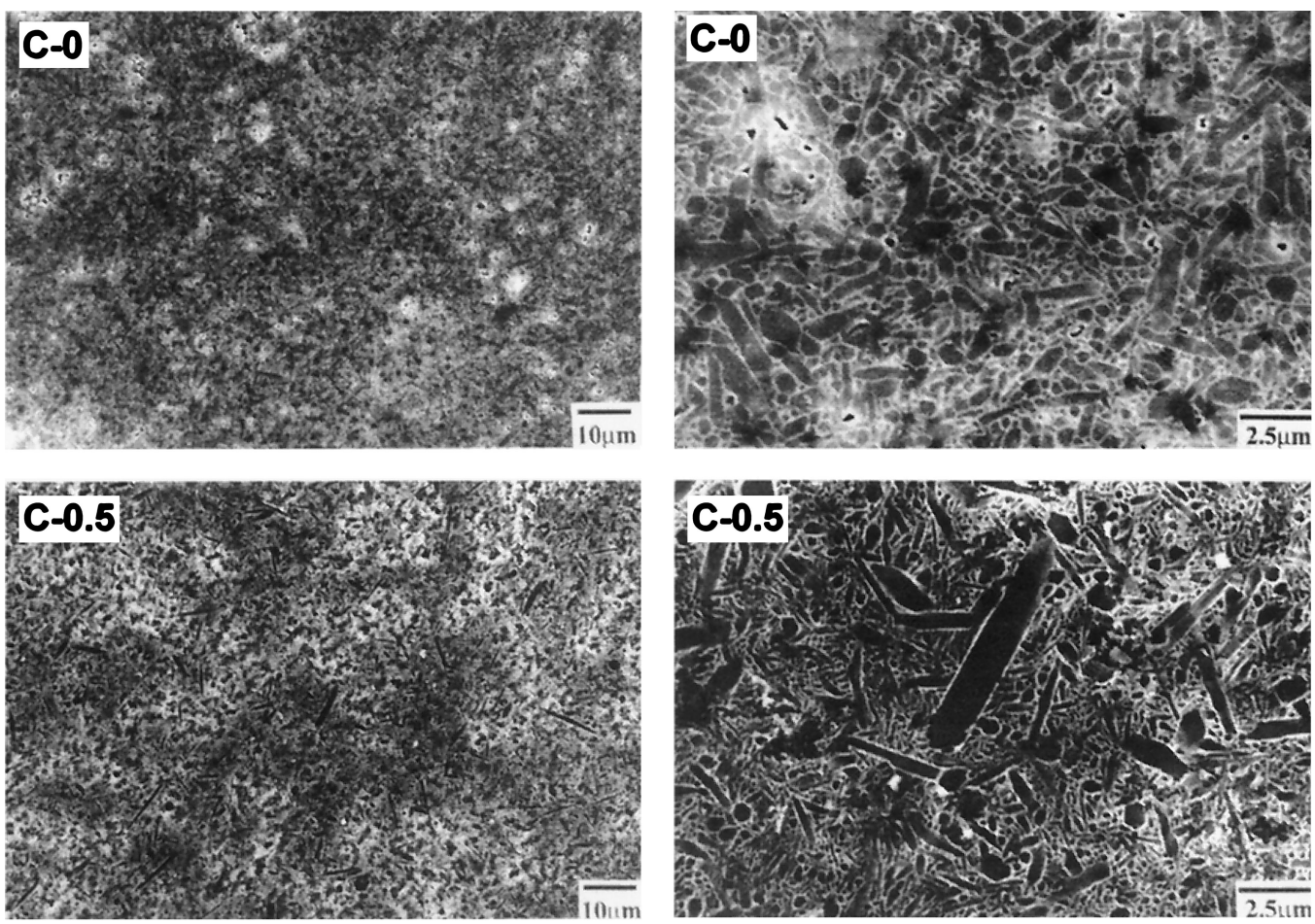

Fig. 3. SEM micrographs for the specimens of C-0 and C-0.5 sintered at 1850°C for 0.5 h. Left side, 1000× magnification; right side, 5000× magnification.

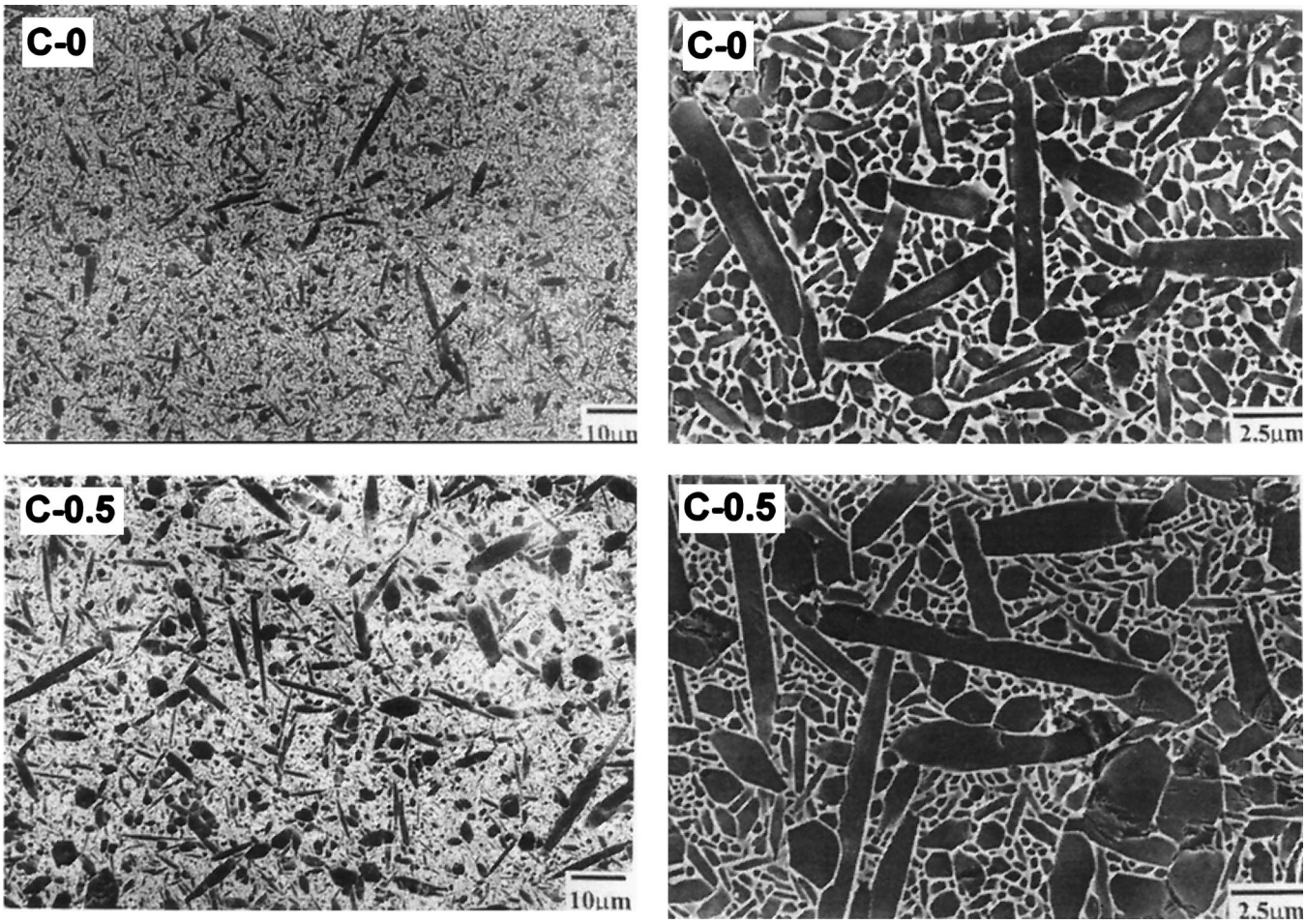

Fig. 4. SEM micrographs for the specimens C-0 and C-0.5 sintered at 1850°C for 3 h. Left side, 1000× magnification; right side, 5000× magnification.

the apatite phase disappears. The disappearance of apatite thus coincides with its melting point, which is 1750°C[28] or 1700°–1800°C.[30]

Both the β-phase content and density increase with increasing temperature and time for the C-0 and C-0.5 specimens after the 1st-step sintering procedure, as shown in Fig. 2. The β-phase content and density for the untreated C-0 specimen are also shown for comparison. C-0 specimens untreated and treated with a 1st-step sintering procedure, such as 1450°C for 10 h under flowing nitrogen gas, show similar behaviors, which suggests that the 1st-step procedure, in the absence of carbon addition, does not produce any significant change in this composition. The α-to-β phase transformation in both the C-0 and C-0.5 specimens is complete at 1750°C. Finally, the phase transformation ratio in the C-0.5 specimens appears to be 10%–20% greater than that observed in the C-0 specimens at temperatures between 1550° to 1650°C.

At a fixed hold time, the C-0 specimen exhibits a continuous increase in density with increasing temperature. At 1850°C, the final stage densification rate of this composition decreases, as is expected if this stage is controlled by diffusion or reaction mechanisms.[20] On the other hand, the carbothermally treated C-0.5 specimen with the apatite phase is expected to have a lower liquid content at <1750°C. This would retard the sintering process, especially those associated with particle rearrangement.[31,32] When the specimen with carbon addition (C-0.5) is treated with the 1st-step sintering procedure (1450°C, 10 h, flowing nitrogen), Y_2O_3–Al_2O_3–SiO_2 eutectic liquid first appears at ~1370°C and wets α-Si_3N_4 particles, which dissolve and produce a Y-Al-Si-O-N glass. Carbon reacts with and reduces the oxygen in the glassy phase, resulting in a rise in the nitrogen:oxygen ratio, and the subsequent precipitation of apatite. After the 1st-step sintering procedure, the specimen consists of α-Si_3N_4, β-Si_3N_4, and apatite as crystalline phases, and should also contain a smaller amount of liquid phase than those without carbon addition. When this specimen is sintered to a higher temperature, such as 1850°C, it will not begin to densify rapidly until a sufficient amount of liquid phase is provided.

Indeed, the observations show that the densification is remarkably suppressed between 1450° to 1750°C for the carbothermally treated C-0.5 specimen. The C-0.5 specimen densities are only 55% and 65% of the theoretical density after heating to 1450° and 1650°C, respectively. For comparison, the specimen without carbon addition has a much higher density of ~85% TD after sintering at 1650°C than would be expected if it contained a sufficiently greater amount of liquid phase. On complete melt of the apatite at or above 1750°C, the amount of liquid phase increases and densification is now promoted, as observed in Fig. 2.

Figures 3, 4, and 5 illustrate the microstructures for the C-0 and C-0.5 specimens that were treated with the 1st-step sintering procedure followed by the 2nd-step sintering at 1850°C for hold times of 0.5, 3, and 6 h, respectively. After sintering at 1850°C for 0.5 h, the dense (97% of the theoretical density) C-0 specimen exhibits a fine-grained microstructure. On the other hand, the C-0.5 specimen contains large elongated grains (Fig. 3).

The density of the C-0.5 specimen sintered at 1750°C for 0.5 h is ~65% of the theoretical density, while that of the C-0 specimen is >85% of the theoretical density. This means that as the temperature begins to increase above 1750°C, there are large pores for β-grains to grow into without being restricted in C-0.5 samples. Thus, when the temperature reaches 1850°C, there are numerous large β-grains in the C-0.5 samples. On the other hand, the C-0 samples are ~90% of the theoretical density at 1750°C, and the growth of β-grains is restricted by grain impingement.

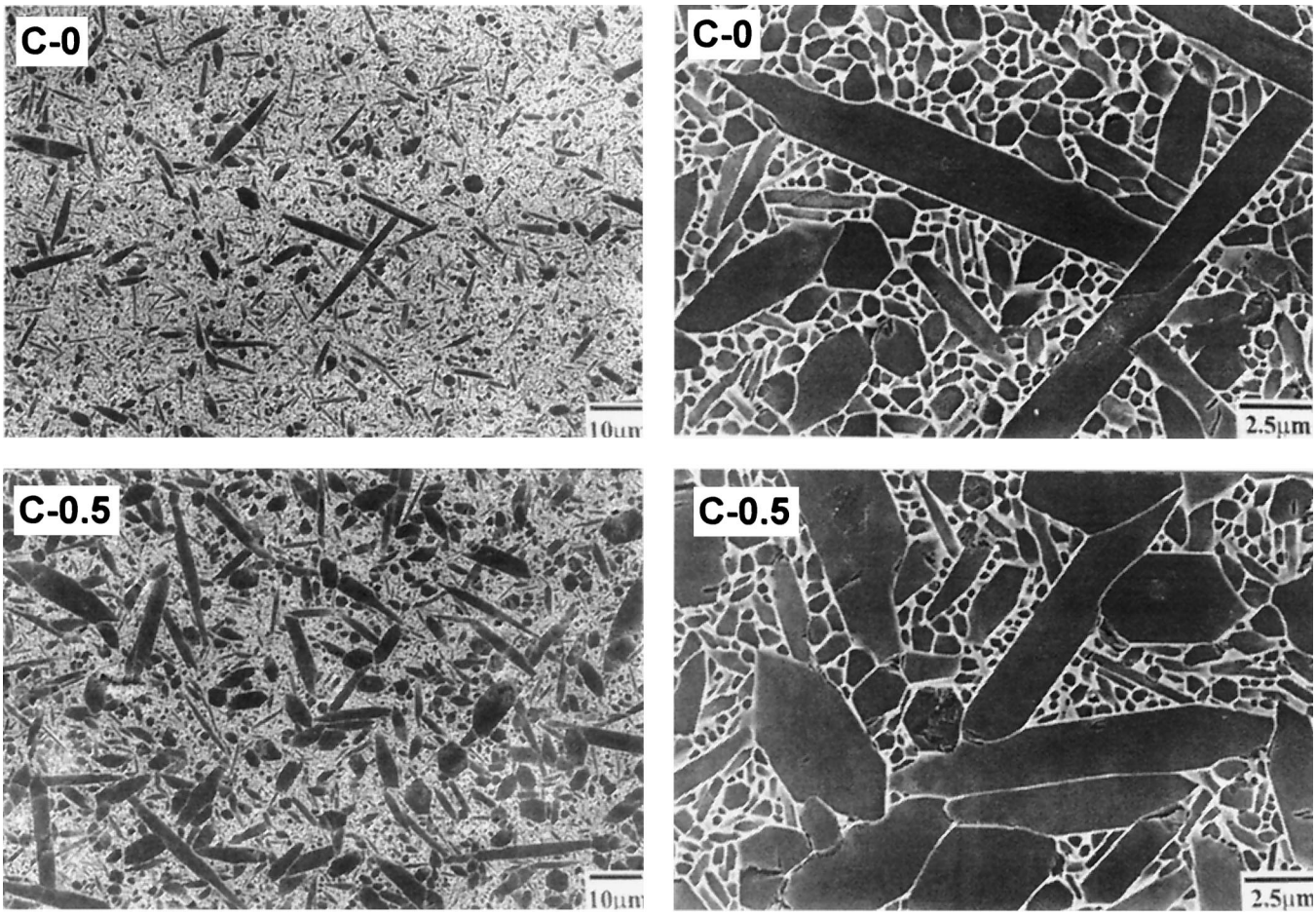

Fig. 5. SEM micrographs for the specimens C-0 and C-0.5 sintered at 1850°C for 6 h. Left side, 1000× magnification; right side, 5000× magnification.

This has been confirmed by investigating the fracture surface of C-0 and C-0.5 specimens sintered at 1750°C, in which large grains are already formed in C-0.5 compared with C-0 (Figs. 6(a) and (b)). It is also possible that the β-particles in the starting powder can start to grow at lower temperatures and could be a source of the large β-grains.

With an increase in sintering time to 3 h, the C-0.5 specimen reaches 98% of the theoretical density accompanied by the continued growth of large elongated grains (Fig. 4). With a further increase in sintering time to 6 h, the diameter of large elongated grains increases while the matrix grains remain fine (Fig. 5).

These microstructures must be a result of a decrease in liquid phase after the 1st-step sintering procedure caused by the formation of the transient apatite phase, which retards densification during the 2nd-step sintering procedure, while allowing the phase transformation to proceed. On melting of this phase at elevated temperatures, the densification and grain growth processes are promoted. Comparison of the quantitative microstructural analysis results for the C-0 and the C-0.5 specimen using the same two-step approach (Fig. 7) confirms that the carbothermal treatment is a key step in achieving the bimodal grain diameter distribution. The present observations suggest that a bimodal microstructure can be achieved without the addition of β-Si_3N_4 seeds by such a two-step process with a carbothermal treatment.

IV. Discussion

To obtain a bimodal microstructure, Mitomo[21] suggested separating the densification from the grain growth process to avoid the concurrent phase transformation, grain growth, and densification processes. A conceptional diagram illustrating three possible cases for the relationship between the densification and the phase transformation is shown in Fig. 8. Included in this diagram are the data of Goto *et al.*[22] for case I and II. In case I, the densification rate is much faster than the α-to-β phase transformation rate, i.e., almost full densification is reached before the α-to-β phase transformation. This can be achieved by hot-pressing compositions with an additive that produces a low viscosity liquid phase. The α-to-β phase transformation during subsequent annealing is used to facilitate the growth of the large β-nuclei that serve as seeds for the grain growth of large β-Si_3N_4 grains. However, it is thought that the control of the number of growing sites is difficult in this case, and growth is limited because of rapid grain impingement in dense materials.

Case II illustrates a system where the densification and the α-to-β phase transformation rates are quite similar, which is commonly encountered with sintering additives such as 5 wt% Y_2O_3 + 2 wt% Al_2O_3, which form a reasonably viscous liquid phase. In this case, densification, grain growth, and the α-to-β phase transformation occur concurrently, which should result in a wide grain size distribution[20] and, thus, the use of β-seed crystals is requisite to obtain bimodal microstructure.[6–9]

Case III represents the approach studied in the present work, in which the densification rate is suppressed while the α-to-β phase transformation is allowed to proceed. Suppression of densification is accomplished by reducing the amount of liquid phase by partial formation of the apatite phase, which results in the retention of high porosity to 1750°C. Apparently, the liquid phase is sufficient to assist in the phase transformation. The overall process provides for a distribution of large β-nuclei in the specimen, which grow during the subsequent higher temperature step and generate a bimodal microstructure. The relationship between the densification and the α-to-β phase transformation for C-0 and C-0.5 specimens sintered at various conditions are plotted in Fig. 9. These results

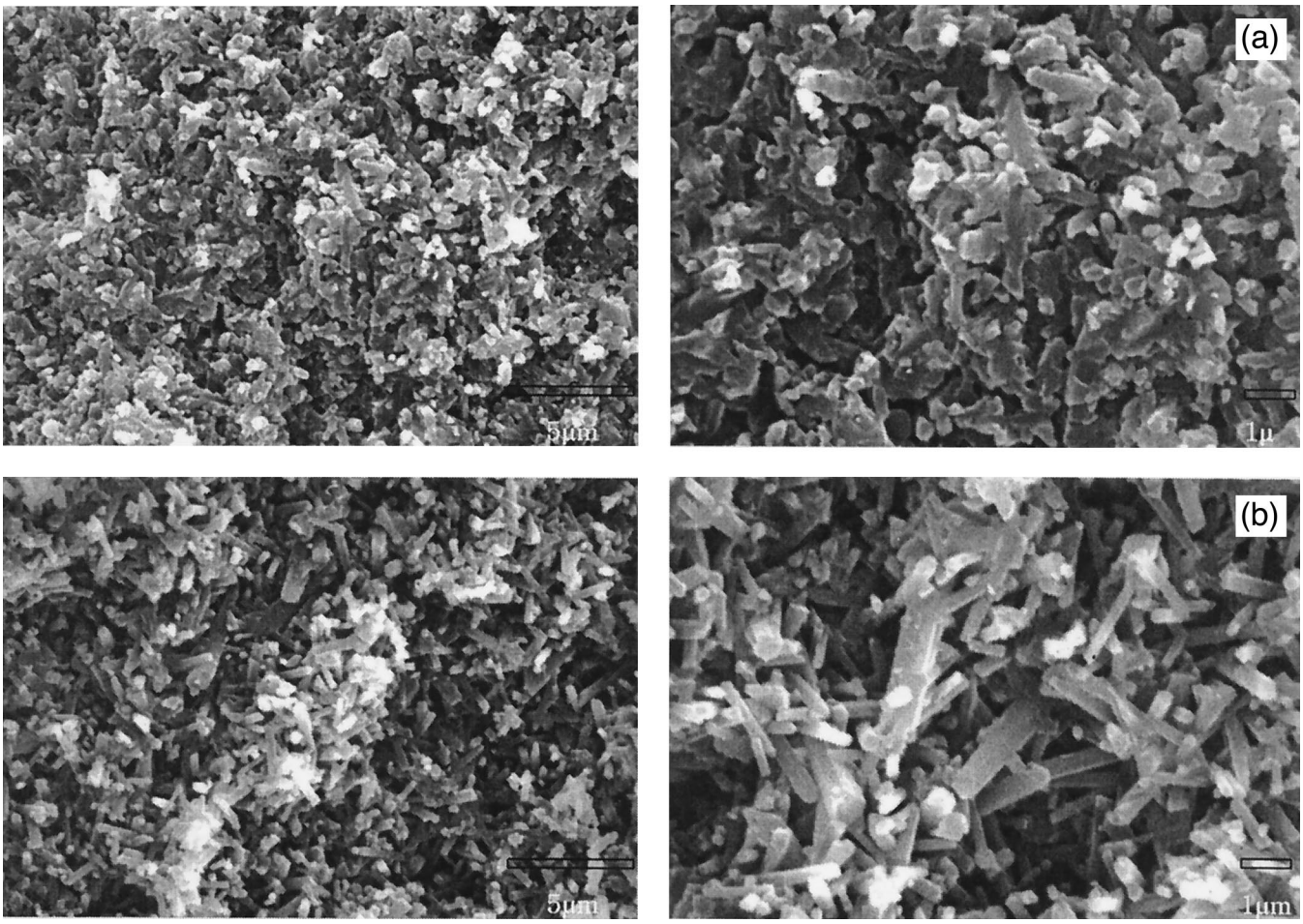

Fig. 6. (a) Fracture surface of C-0 specimen sintered at 1750°C (~90% TD, ~100% β/(α+β)). Low magnification (left), high magnification (right). (b) Fracture surface of C-0.5 specimen sintered at 1750°C (~67% TD, ~100% β/(α+β)). Left, low magnification; right, high magnification.

clearly show that the carbothermal reduction treatment followed by a high-temperature sintering effectively suppresses the densification process and allows the α-to-β phase transformation to proceed at intermediate temperatures. The deviation from the linear relationship for case II between data points in Figs. 8 and 9 originates from the different sintering additives (e.g., 5Y2A in Fig. 8 and 6Y1A in Fig. 9).

The carbothermal reduction process or the use of carbon in Si_3N_4 technology has been widely investigated to (i) produce Si_3N_4 powder at a relatively inexpensive price,[33–36] (ii) reduce the surface silica content,[37] (iii) investigate the effect of remaining carbon content on the densification process,[38,39] and (iv) investigate the effect of oxynitride crystalline phases such as apatite, wallastonite, or melilite on the creep properties of Si_3N_4.[40,41] In general, excess carbon is detrimental in densification, and SiC forms above ~1500°C and inhibits the sintering behavior.[35,36,39] In the present experiments, the amount of carbon left after the carbothermal reduction treatment is only ~0.1%, which is the comparable amount to that in the starting Si_3N_4 powder. Thus, the added carbon is consumed in the process of reducing the oxygen content during the carbothermal reduction treatment.

During the gas pressure sintering step, the α-to-β phase transformation for the C-0.5 specimen was faster than that of the C-0 specimen at temperatures between 1550° to 1650°C. At the same time, the degree of the α-to-β phase transformation just after the carbothermal reduction process was also higher in C-0.5 specimens than in C-0 specimens. This higher initial β-content is likely one of the sources of the faster transformation in the C-0.5 specimen, while an increasing temperature as the phase transformation rate is known to be dependent on the number of β-nuclei present.[42,43] Ordonez *et al.*[44] studied the sintering and phase transformation of Si_3N_4 with SiO_2 and Y_2O_3–SiO_2 additives and showed that phase transformation is faster with a smaller amount of liquid phase, although the detailed mechanism was not suggested. When a small amount of liquid phase is available, it is easier to be saturated with nitrogen to produce faster precipitation to β-Si_3N_4. This result might support the diffusion mechanism operative in the system investigated. This result is inconsistent with that of Lee *et al.*,[45] in which phase transformation and grain growth are operative by interfacial reaction. The diffusion mechanism will be more pronounced when the liquid content is very small.

When there is enough liquid phase present, heterogeneous nucleation occurs very rapidly as the temperature increases, and can produce an uncontrollable grain growth of β-nuclei of a variety of sizes. This is avoided by limiting the amount of liquid phase.

V. Conclusions

(1) The carbothermal reduction treatment of powder compacts of a mixture of Si_3N_4, sintering additives, and a carbon mixture at 1450°C depletes the oxygen content in the Y-Si-Al-O-N glass formed, and, as a result, leads to the precipitation of crystalline oxynitride phases such as apatite during the 1st-step sintering procedure.

(2) Precipitation of the apatite phase suppresses the densification process effectively by reducing the amount of liquid phase present at an intermediate temperature region during the 2nd-step sintering procedure. The α-to-β phase transformation is complete at 1750°C.

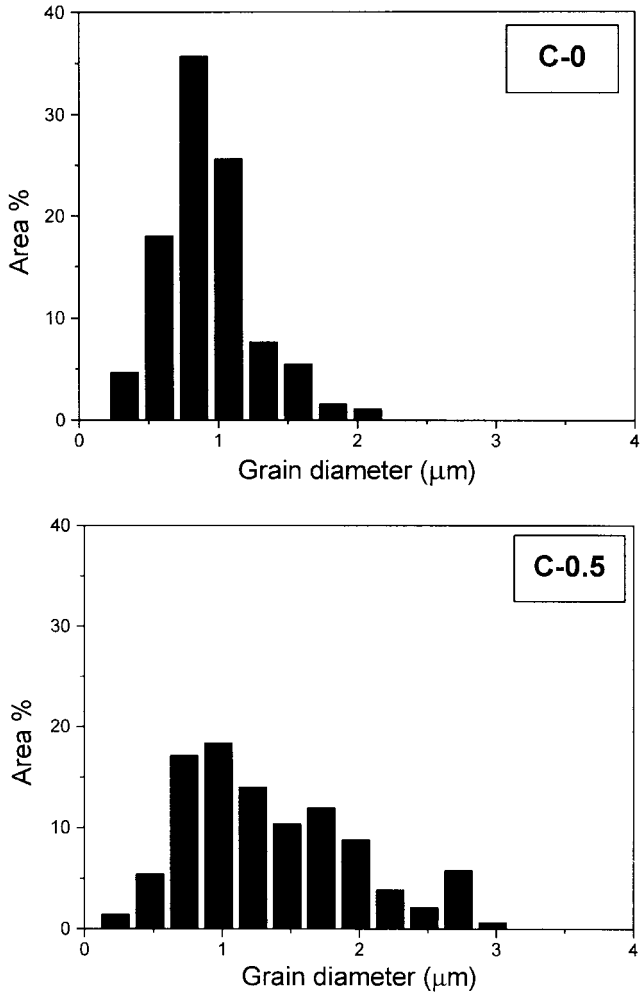

Fig. 7. Distribution of grain diameter for C-0 and C-0.5 specimens sintered at 1850°C for 3 h under 1 MPa of nitrogen pressure.

(3) At or near 1750°C, the apatite phase melts, producing a sufficient liquid phase to accelerate densification and the growth of large reinforcing grains, which leads to a bimodal microstructure.

(4) The suppression of the densification process, while the α-to-β phase transformation is not hindered, provides a favorable situation for a selective grain growth of large β-nuclei to grow to the large elongated grains, which can act as reinforcing grains.

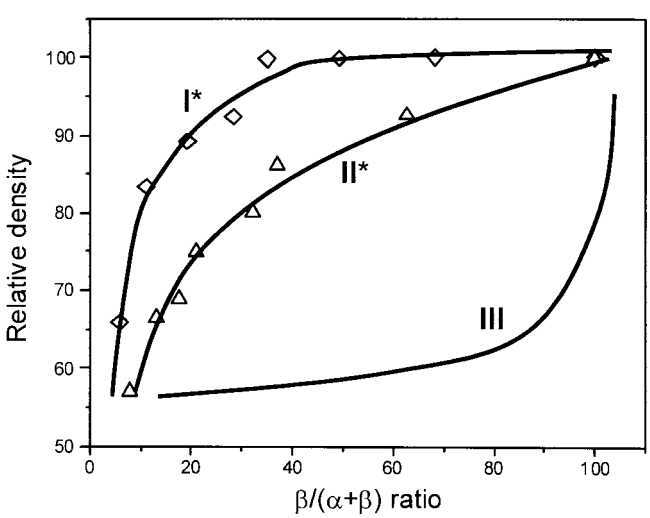

Fig. 8. Schematic diagram of the relationship between the densification and the phase transformation, showing three different cases ((◇) system 1Y6A and (△) system 5Y2A). (*See Ref. 22.)

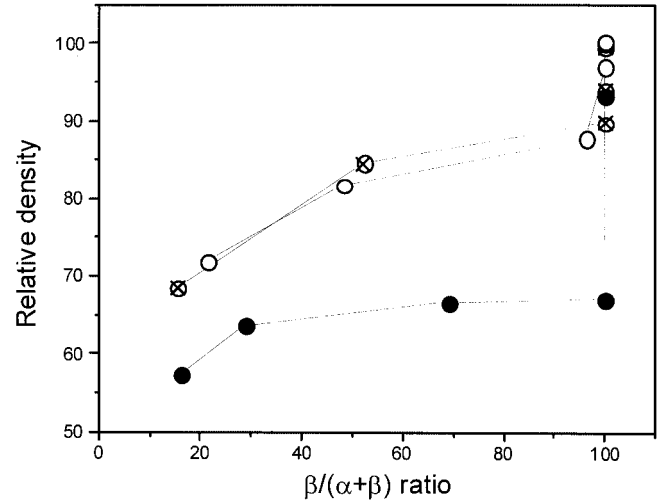

Fig. 9. Relationship between the densification and phase transformation for C-0 specimens (⊗) without the 1st-step sintering procedure and (○) with the 1st-step sintering procedure and (●) C-0.5 specimens sintered under various conditions.

References

[1]P. F. Becher, "Microstructural Design of Toughened Ceramics," *J. Am. Ceram. Soc.*, **74** [2] 255–69 (1991).

[2]P. F. Becher, S.-L. Hwang, and C.-H. Hsueh, "Using Microstructure to Attack the Brittle Nature of Silicon Nitride Ceramics," *MRS Bull.*, **20** [2] 23–27 (1995).

[3]P. F. Becher, E. Y. Sun, K. P. Plucknett, K. B. Alexander, C.-H. Hsueh, H.-T. Lin, S. B. Waters, C. G. Westmoreland, E.-S. Kang, K. Hirao, and M. E. Brito, "Microstructural Design of Silicon Nitride with Improved Fracture Toughness, Part 1: Effect of Grain Size and Shape," *J. Am. Ceram. Soc.*, **81** [11] 2821–30 (1998).

[4]E. Y. Sun, P. F. Becher, K. P. Plucknett, C.-H. Hsueh, K. B. Alexander, S. B. Waters, K. Hirao, and M. E. Brito, "Microstructural Design of Silicon Nitride with Improved Fracture Toughness, Part 2: Effect of Yttria and Alumina Additives," *J. Am. Ceram. Soc.*, **81** [11] 2831–40 (1998).

[5]P. F. Becher, C.-H. Hsueh, K. B. Alexander, and E. Y. Sun, "Influence of Reinforcement Content and Diameter on the R-Curve Response in SiC-Whisker-Reinforced Alumina," *J. Am. Ceram. Soc.*, **79** [2] 298–304 (1996).

[6]K. Hirao, T. Nagaoka, M. E. Brito, and S. Kanzaki, "Microstructure Control of Silicon Nitride by Seeding with Rodlike Beta Silicon Nitride Particles," *J. Am. Ceram. Soc.*, **77** [7] 1857–62 (1994).

[7]K. Hirao, M. Ohashi, M. E. Brito, and S. Kanzaki, "Processing Strategy for Producing Highly Anisotropic Silicon Nitride," *J. Am. Ceram. Soc.*, **78** [6] 1687–90 (1995).

[8]T. Ohji, K. Hirao, and S. Kanzaki, "Fracture Resistance Behavior of Highly Anisotropic Silicon Nitride," *J. Am. Ceram. Soc.*, **78** [11] 3125–28 (1995).

[9]K. Hirao, K. Watari, M. E. Brito, M. Toriyama, and S. Kanzaki, "High Thermal Conductivity in Silicon Nitride with Anisotropic Microstructure," *J. Am. Ceram. Soc.*, **79** [9] 2485–88 (1996).

[10]W. Dressler, H.-J. Kleebe, M. J. Hoffmann, M. Ruehle, and G. Petzow, "Model Experiments Concerning Abnormal Grain Growth in Silicon Nitride," *J. Eur. Ceram. Soc.*, **16**, 3–14 (1996).

[11]M. Mitomo, "Design and Processing for Silicon Nitride In-Situ Composite"; pp. 85–90 in *6th International Symposium on Ceramic Materials and Components for Engines* (Oct. 1997). Edited by K. Niihara, S. Konzaki, K. Komeya, S. Hirano, and K. Morinaga. Technoplaza Co. Ltd., Arita, Japan, 1997.

[12]N. Hirosaki, Y. Akimune, and M. Mitomo, "Microstructure Characterization of Gas-Pressure-Sintered Beta-Silicon Nitride Containing Large Beta-Silicon Nitride Seeds," *J. Am. Ceram. Soc.*, **77** [4] 1093–97 (1994).

[13]H. Emoto and M. Mitomo, "Control and Characterization of Abnormally Grown Grains in Silicon Nitride Ceramics," *J. Eur. Ceram. Soc.*, **17**, 797–804 (1997).

[14]P. Sajgalik, J. Dusza, and M. J. Hoffmann, "Relationship Between Microstructure, Toughening Mechanisms, and Fracture Toughness of Reinforced Silicon Nitride Ceramics," *J. Am. Ceram. Soc.*, **78** [10] 2619–24 (1995).

[15]T. Hirano, J. Yang, and K. Niihara, "Effect of Seed Crystal Properties on the Microstructure of Si_3N_4 Ceramics," *J. Ceram. Soc. Jpn.*, **104** [5] 462–65 (1995).

[16]K. Hirao, A. Tsuge, M. E. Brito, and S. Kanzaki, "Preparation of Rod-Like Beta Silicon Nitride Single Crystal Particles," *J. Ceram. Soc. Jpn., Int. Ed.*, **101,** 1051–52 (1993).

[17]K. Furuya, K. Matsuo, F. Munakata, Y. Akimune, J. Je, Y. Yamamoto, and I. Ishikawa, "Synthesis of Large-Size β-Si_3N_4 Crystals," *J. Mater. Res.*, **14** [5] 1690–91 (1999).

[18]S. Kanzaki, K. Hirao, M. E. Brito, K. Watari, M. Toriyama, H. Imamura, and M. Kitayama, "Development of High Performance Si_3N_4 through Textured Microstructure Control"; presented at the 100th Annual Meeting of the American Ceramic Society, Cincinnati, OH, 1998.

[19]P. D. Ramesh, R. Oberacker, and M. J. Hoffmann, "Preparation of β-Silicon Nitride Seeds for Self-Reinforced Silicon Nitride Ceramics," *J. Am. Ceram. Soc.*, **82** [6] 1608–10 (1999).

[20]M. Mitomo and M. Uenosono, "Microstructural Development during Gas-Pressure Sintering of Alpha-Silicon Nitride," *J. Am. Ceram. Soc.*, **75** [1] 103–108 (1992).

[21]M. Mitomo, "In-Situ Microstructural Control in Engineering Ceramics," *Key Eng. Mater.*, **161–163**, 53–58 (1999).

[22]Y. Goto and G. Thomas, "Phase Transformation and Microstructural Changes of Si_3N_4 during Sintering," *J. Mater. Sci.*, **30**, 2194–200 (1995).

[23]C. P. Gazzara and D. R. Messier, "Determination of Phase Content of Si_3N_4 by X-Ray Diffraction Analysis," *Am. Ceram. Soc. Bull.*, **56** [9] 777–81 (1977).

[24]U. Kolitsch, H. J. Seifert, T. Ludwig, and F. Aldinger, "Phase Equilibria and Crystal Chemistry in the Y_2O_3-Al_2O_3-SiO_2 System," *J. Mater. Res.*, **14** [2] 447–55 (1999).

[25]L. C. Pathak, A. K. Ray, S. Das, C. S. Sivaramakrishnan, and P. Ramachandrarao, "Carbothermal Synthesis of Nanocrystalline Aluminum Nitride Powders," *J. Am. Ceram. Soc.*, **82** [1] 257–60 (1999).

[26]F. F. Lange, S. C. Singhal, and R. C. Kuznicki, "Phase Relations and Stability Studies in the Si_3N_4-SiO_2-Y_2O_3 Pseudoternary System," *J. Am. Ceram. Soc.*, **60** [5–6] 249–52 (1977).

[27]K. H. Jack, "Sialons: A study in Materials Development," pp. 1–30 in *Non-Oxide Technical and Engineering Ceramics*. Edited by S. Hampshire. Elsevier Applied Science, London, U.K., 1986.

[28]L. J. Gauckler, H. Hohnke, and T. Y. Tien, "The System Si_3N_4-SiO_2-Y_2O_3," *J. Am. Ceram. Soc.*, **63** [1–2] 35–37 (1980).

[29]R. R. Wills, "Reaction of Si_3N_4 with Al_2O_3 and Y_2O_3," *J. Am. Ceram. Soc.*, **58** [7–8] 335 (1975).

[30]H.-J. Kleebe and G. Ziegler, "Influence of Crystalline Secondary Phases on the Densification Behavior of Reaction-Bonded Silicon Nitride during Postsintering under Increased Nitrogen Pressure," *J. Am. Ceram. Soc.*, **72** [12] 2314–17 (1989).

[31]W. D. Kingery, "Densification during Sintering in the Presence of a Liquid Phase: I. Theory," *J. Appl. Phys.*, **30** [3] 301–06 (1959).

[32]W. D. Kingery and M. D. Narasimhan, "Densification during Sintering in the Presence of a Liquid Phase: II. Experimental," *J. Appl. Phys.*, **30** [3] 307–10 (1959).

[33]I. H. Kang, K. Komeya, T. Meguro, M. Naito, and O. Hayakawa, "Effect of Silicon Nitride Seeds Addition on the Particle Size and the Crystal Form of Resulting Powder in Carbothermal Reduction–Nitridation of Silica," *J. Ceram. Soc. Jpn.*, **104** [6] 471–75 (1996).

[34]P. Petrovski, H. Smailhodzis, and S. Maric, "Preparation of Silicon Oxynitride and Nitride by Nitridation of Amorphous Silica in Ammonia," *Mater. Sci. Eng., A*, **109**, 265–69 (1989).

[35]M. Ekelund and B. Forslund, "Carbothermal Preparation of Silicon Nitride: Influence of Starting Material and Synthesis Parameters," *J. Am. Ceram. Soc.*, **75** [3] 532–39 (1992).

[36]R. Koc and S. Kaza, "Synthesis of Alpha Silicon Nitride from Carbon Coated Silica by Carbothermal Reduction and Nitridation," *J. Eur. Ceram. Soc.*, **18**, 1471–77 (1998).

[37]A. W. Weimer, D. F. Carroll, D. W. Susnitzky, and D. R. Beaman, "Morphology and Sinterability of Thermally Treated Carbothermally Synthesized Silicon Nitride Powders," *J. Am. Ceram. Soc.*, **82** [6] 1635–38 (1999).

[38]S. Wada, M. Suganuma, Y. Kitagawa, and N. Murayama, "Delay of α to β Transformation of Si_3N_4 Contacting with Carbon during Hot-Pressing and PECS," *J. Ceram. Soc. Jpn.*, **106** [9] 924–26 (1998).

[39]K. Watari, M. Kawamoto, and K. Ishizaki, "Carbon Behavior in Sintered Silicon Nitride Grain Boundaries," *Mater. Sci. Eng., A*, **109**, 89–95 (1989).

[40]S. Hampshire and K. H. Jack, "The Effect of Carbon Content of Silicon Nitride on the Subsequent Oxidation of Phases in the Y-Si-O-N System," pp. 350–57 in *Proceedings of the International Symposium on Ceramic Components for Engines*. Edited by S. Sōmiya, E. Kanai, and K. Ando. KTK Scientific, Tokyo, Japan, 1984.

[41]H. Knoch and G. E. Gazza, "Effect of Carbon Impurity on the Thermal Degradation of a Si_3N_4–Y_2O_3 Ceramic," *J. Am. Ceram. Soc.*, **62** [11–12] 634–35 (1979).

[42]T. N. Tiegs, F. C. Montgomery, J. L. Schroeder, D. L. Barker, and P. A. Menchhofer, "Effect of Powder Characteristics on the Alpha to Beta Silicon Nitride Transformation Kinetics," *Ceram. Eng. Sci. Proc.*, **18** [4] 437–47 (1997).

[43]G. Ziegler, J. Heinrich, and G. Woetting, "Review: Relationship between Processing, Microstructure and Properties of Dense and Reaction-Bonded Silicon Nitride," *J. Mater. Sci.*, **22**, 3041–86 (1987).

[44]S. Ordonez, I. Iturriza, and F. Castro, "The Influence of Amount and Type of Additives on α→β Si_3N_4 Transformation," *J. Mater. Sci.*, **34**, 147–53 (1999).

[45]D. D. Lee, S.-J. L. Kang, and D. N. Yoon, "Mechanism of Grain Growth and α-β′ Transformation during Liquid-Phase Sintering of β′-Sialon," *J. Am. Ceram. Soc.*, **71** [9] 803–806 (1988).

[46]Powder Diffraction File. International Centre for Diffraction Data, Newtown Square, PA. □